Published in final edited form as:
*Structure*. 2014 June 10; 22(6): 819–829. doi:10.1016/j.str.2014.04.002.

# KEY INTERACTIONS FOR CLATHRIN COAT STABILITY

**Till Böcking**[1,4,*], **Francois Aguet**[1], **Iris Rapoport**[1,3], **Manuel Banzhaf**[1,3], **Anan Yu**[1,3,5], **Jean Christophe Zeeh**[1,3], and **Tom Kirchhausen**[1,2,3,*]

[1]Department of Cell Biology, Harvard Medical School, Boston, Massachusetts, 02115, USA

[2]Department of Pediatrics, Harvard Medical School, Boston, Massachusetts, 02115, USA

[3]Program in Cellular and Molecular Medicine at Boston Children's Hospital, Boston, Massachusetts, 02115, USA

[4]Centre for Vascular Research, University of New South Wales, Sydney 2052 Australia

## SUMMARY

Clathrin-coated vesicles are major carriers of vesicular traffic in eukaryotic cells. This endocytic pathway relies on cycles of clathrin coat assembly and Hsc70-mediated disassembly. Here we identify histidine residues as major determinants of lattice assembly and stability. They are located at the invariant interface between the proximal and distal segments of clathrin heavy chains, in triskelions centered on two adjacent vertices of the coated-vesicle lattice. Mutation of these histidine to glutamine alters the pH dependence of coat stability. We then describe single-particle fluorescence imaging experiments in which we follow the effect of these histidine mutations on susceptibility to Hsc70-dependent uncoating. Coats destabilized by these mutations require fewer Hsc70 molecules to initiate disassembly as predicted by a model in which Hsc70 traps conformational distortions during the auxilin- and Hsc70:ATP-mediated uncoating reaction.

## INTRODUCTION

In eukaryotic cells, clathrin coated vesicles mediate internalisation of cargo molecules such as nutrients, hormones and lipoproteins. Clathrin assembles on the intracellular surface of the plasma membrane into closed lattices that drive membrane invagination (Brodsky et al., 2001; Edeling et al., 2006; Kirchhausen, 2000). After budding from the plasma membrane, the coated vesicle must rapidly shed its clathrin coat to allow fusion of the naked vesicle with its endosomal targets and recycling of coat components. This 'uncoating' process is catalysed by heat shock cognate protein 70 (Hsc70) (Schlossman et al., 1984), a molecular



*Correspondence: till.boecking@unsw.edu.au or kirchhausen@crystal.harvard.edu.
[5]Present address: Department of Molecular Biosciences, Rice Institute for Biomedical Research, Northwestern University, Evanston, Illinois, 60208, USA

**CONFLICT OF INTEREST**
The authors declare that they have no conflict of interest.

chaperone that is recruited to the coated vesicle by its co-chaperone auxilin (Ungewickell et al., 1995). The timing of the uncoating reaction is determined by the association of auxilin with the coated vesicle just after scission from the membrane (Guan et al., 2010; Massol et al., 2006). Hsc70 functions as a simple ATP-driven molecular clamp that goes through cycles of substrate binding and release (Hartl and Hayer-Hartl, 2009). In the ATP-loaded state, its substrate binding domain is in an open conformation and binds to clathrin with fast on-rate and low affinity. ATP hydrolysis, triggered by interaction with the J-domain of auxilin and with its substrate, is coupled to a conformational change in the substrate binding domain, resulting in a closed conformation and tight clathrin binding. Nucleotide exchange resets the cycle and leads to reopening of Hsc70 and substrate release. This process is catalysed by nucleotide exchange factors such as Hsp110, which facilitates Hsc70-driven clathrin uncoating by promoting the dissociation of the Hsc70/ADP-clathrin complex (Morgan et al., 2013; Schuermann et al., 2008).

Our knowledge of the interactions involved in clathrin coat stability and disassembly is largely based on reconstitution of these processes *in vitro*. The basic assembly unit of the coat is the clathrin triskelion, a pinwheel-shaped molecule consisting of three ~190 kDa heavy chain ‘legs’ radiating from a trimeric hub and each associated with a ~30 kDa light chain (Figure 1). Purified clathrin triskelions self-assemble at slightly acidic pH into ‘cages’ ranging in diameter from ~50–120 nm (Kirchhausen and Harrison, 1981; Pearse and Crowther, 1987). Clathrin adaptor proteins facilitate self assembly (Keen, 1990), and the resulting structures, termed ‘coats’, exhibit a narrower size distribution than do empty cages assembled without adaptor proteins (Pearse and Crowther, 1987). The structure of the hexagonal D6 barrel coat (Figure 1), assembled from clathrin and a fraction containing the heterotetrameric adaptor protein AP-2, has been obtained by electron cryomicroscopy (cryoEM) (Fotin et al., 2004b; Musacchio et al., 1999; Smith et al., 1998; Vigers et al., 1986). The “hub” of a triskelion (clathrin residues 1074-1675) is centred at each vertex of the coat. Each edge in the outer shell of the coat consists of two proximal legs from neighbouring triskelions (Figure 1A), each with a distal leg from another triskelion running just below it. The extended radial contact between the parallel proximal and distal leg (Figure 1B) is the most extensive interface in the lattice and is invariant among coat structures with and without bound chaperones, suggesting that it determines the stability of the coat (Fotin et al., 2004b; Xing et al., 2010). The specific residues involved in stabilising the clathrin coat have not yet been identified. The stability of the clathrin lattice is strongly pH dependent. At pH 6.0 clathrin cages and coats are very stable and even resist Hsc70-driven uncoating (Braell et al., 1984; Schmid and Rothman, 1985; Xing et al., 2010); at pH 7.5, the clathrin lattice spontaneously depolymerises (Pearse and Crowther, 1987). This pH dependence implicates the involvement histidine residues, which have a pKa between 6.3 – 6.9.

Insight into the mechanism of Hsc70-driven clathrin coat disassembly comes from structural and biochemical studies of *in vitro* assembled clathrin coats. Up to three auxilin molecules bind beneath each vertex, where each auxilin associates with a terminal domain of a clathrin heavy chain and also makes contact with the ankle segments of two other triskelions (Fotin et al., 2004a). Auxilin positions Hsc70 on the inside of the coat, close to the inward

projecting C-terminal tripod formed by an extended helix from each heavy chain. In this location Hsc70 can bind to a QLMLT consensus motif in the C-terminal unstructured region of clathrin heavy chain required for the uncoating reaction (Rapoport et al., 2008). A cryoEM reconstruction of an uncoating intermediate trapped at low pH shows that Hsc70 binds on the inner surface of the intact coat with a stochiometry of approximately one molecule per vertex (Xing et al., 2010). Hsc70 binding leads to a distortion of the lattice (Xing et al., 2010). Using fluorescence microscopy we have followed the uncoating reaction in real time (Böcking et al., 2011). In conjunction with the lattice distortion observed in the cryoEM structure (Xing et al., 2010) we proposed a model in which Hsc70 molecules capture multiple destabilising fluctuations of clathrin molecules for long enough to reinforce each other and lead to coat disassembly.

In the work described here, we have identified histidine residues at the interface of proximal and distal segments of clathrin heavy chains in a coat and show that mutating sets of these residues to glutamine destabilizes the coat. We have systematically altered the stability of the clathrin coat by exploiting its well-known pH sensitivity (Barouch et al., 1997; Braell et al., 1984; Schmid and Rothman, 1985) or by mutating the identified histidine residues to determine the effect of coat stability on the kinetics of the Hsc70-driven uncoating reaction. Using fluorescence microscopy and kinetic modelling we show that coats destabilized by mutation of certain histidine residues require fewer Hsc70 molecules to initiate disassembly.

## RESULTS

### Role of histidine residues in coat stability

We identified six candidate histidine residues from the cryoEM structure of the clathrin coat (Fotin et al., 2004a) that might participate in electrostatic interactions and/or hydrogen bonds in the clathrin lattice. Residues H867 and H876 in the distal leg segment and residues H1275, H1279, H1432 and H1458 in the proximal leg segment are at the proximal-distal interface (see Figure 1 for details). Using the crystal structure of the heavy chain residues 1210-1516 (Ybe et al., 1999) we further confirmed that the imidazole rings of the four candidate histidine residues in the proximal segment are oriented towards the interface with the distal segment. To test whether these residues are involved in stabilising the coat, we generated three histidine to glutamine double mutants of rat clathrin heavy chain (H867Q/H876Q, H1275Q/H1279Q and H1432Q/H1458Q, designated H8, H12 and H14, respectively). In addition we generated a quadruple mutant by combining the double mutants H12 and H14 (designated 4×H→Q) and a sextuple mutant combining all three double mutants (designated 6×H→Q). Mutant clathrin heavy chains were expressed in insect cells and purified as triskelions. We then added recombinant clathrin light chain LCa1 to the purified heavy chain to reconstitute triskelions containing three heavy and three light chains.

We verified that both wild type and mutant clathrin triskelions assemble into coats by *in vitro* association with an adaptor fraction highly enriched in the heterotetrameric clathrin adaptor AP-2; we refer to these coats as clathrin/AP-2 coats. SDS PAGE analysis of the high speed pellets collected after coat formation at pH 6.5 revealed that wild type and mutant triskelions formed assemblies that co-sedimented with AP-2 (Figure 2A). Clathrin light chain bound at similar or only slightly reduced levels (~70–95%) to mutant clathrin coats

compared to wild type clathrin coats as estimated by densitometry of Coomassie-stained gels of several coat preparations. The yield of coats for the three double mutants H8, H12 and H14 were comparable to wild type. Negative-stain electron micrographs of the resuspended pellets showed that these mutants formed coats with an appearance and diameter (~68–69 nm) indistinguishable from the D6 barrel coats formed by wild type clathrin (Figure 2B and C) (Fotin et al., 2004b; Smith et al., 1998; Xing et al., 2010). The 4×H→Q mutants assembled into homogeneous structures with an average diameter of ~60 nm, significantly smaller than wild type coats (Figure 2B and C), and we therefore did not include these coats in further studies. Resuspended pellets of structures formed with clathrin triskelions containing all six histidine to glutamine mutations contained very few assembled structures; electron micrographs showed mainly free triskelions (Figure 2B). We conclude that the assemblies formed at high concentrations of 6×H→Q clathrin and AP-2 (see Figure 1) dissociated rapidly upon resuspension of the high speed pellet at pH 6.5.

We devised a simple fluorescence microscopy assay to compare the stability of wild type and mutant clathrin coats by measuring the loss of fluorescent triskelions from coats exposed to buffer solutions of increasing pH (Figure 3A). Spontaneous, uncatalysed disassembly of *in-vitro* clathrin structures occurs after dilution below a critical threshold (Crowther and Pearse, 1981; Kirchhausen and Harrison, 1981). We predicted that coats assembled with clathrin lacking residues involved in stabilising the lattice would fall apart more readily with increasing pH than do wild type coats. Wild type coats labelled with Alexa Fluor 488 and histidine double mutant coats labelled with DyLight 649 were captured onto the same cover slip for observation by total internal reflection microscopy. Using microfluidic delivery, the coats were then exposed successively to buffer solutions of increasing pH and imaged one minute after each solution exchange to determine the fluorescence intensity remaining for each type of coat.

A representative series of images comparing wild type and H8 mutant coats in the range from pH 6.4 to pH 7.8 is shown in Figure 3B. From the images it was immediately apparent that the mutant coats (red) disappeared at a lower pH threshold than wild type coats. Individual coat signals within each population decreased to varying degrees at each pH step (Figure S1), as expected for coats with variable contents of AP-2. The mean signal intensity relative to the signal at pH 6.4 for wild type and mutant coats after each pH step is shown in Figure 3C. Wild type coats dissociated to limited extent up to pH 7.2 with minor decreases in the coat intensity after each step. At pH 7.4 most of the wild type coat signal was lost rapidly; the signal reached background levels at pH 7.6. For coats assembled with histidine double mutants H8, H12 and H14, the fluorescence signal had fallen to about half its initial value at pH 6.2 when the pH reached pH 6.8 (Figure 3C). At pH 7.0 the mutant coats had essentially disappeared while the wild type coats were still largely intact. We conclude that histidine residues located at the interface between proximal and distal leg segments contribute to stabilising contacts in the clathrin lattice.

### Uncoating reaction with destabilised H14 clathrin/AP-2 coats

Our model for Hsc70-driven uncoating predicts that to dissociate coats destabilized by mutation would require fewer Hsc70 molecules than needed to dissociate wild-type coats.

We used our single particle fluorescence microscopy uncoating assay (Böcking et al., 2011) to measure chaperone binding and coat disassembly for individual coats (Figure 4): Fluorescent clathrin/AP-2 coats were captured onto a modified glass coverslip and immediately incubated with auxilin(547-910). Auxilin binding stabilised the clathrin coat (Ahle and Ungewickell, 1990; Scheele et al., 2001) and slowed the spontaneous dissociation of the H14 lattices; the auxilin(547-910)-loaded H14 coats remained intact at pH 6.8 (Figure 4E) in the absence of Hsc70-ATP. We then initiated the uncoating reaction by injecting a solution containing auxilin(547-910), Hsc70 and ATP into the flow channel while measuring the fluorescence intensities of the clathrin- and Hsc70-associated signals by time-lapse TIRF microscopy with alternating fluorescence excitation. Wild type and H14 mutant coats appeared in the fluorescence image as bright, diffraction-limited spots (Figure 4B, top row) which persisted after addition of Hsc70-ATP for varying periods of time before disappearing rapidly as a result of coat disassembly (Figure 4B, bottom row and 4C). The onset of signal decay varied among individual coats in the population but occurred on average earlier for H14 mutant than wild type coats.

Clathrin and Hsc70 fluorescence intensity traces extracted from the time-lapse images for each coat in the field of view exhibited typical uncoating kinetics (Böcking et al., 2011) for the wild-type coats (Figure 4D, wt): During an accumulation phase, the clathrin signal remained constant while the Hsc70 signal increased steadily. The clathrin- and Hsc70-associated signals started abruptly to decline to background at about the time at which the Hsc70 signal had reached its maximum. A small signal remained at the location of the coat in each channel corresponding to the clathrin bound to the antibody on the coverslip surface and associated Hsc70 molecules. The H14 intensity traces (Figure 4B, H14) showed the same basic uncoating behaviour characterised by an accumulation and a disassembly phase but with on average shorter accumulation times as expected for the destabilised H14 clathrin lattice.

We used our kinetic model for the Hsc70-driven uncoating reaction (Figure 5A, (Böcking et al., 2011)) to calculate the number of Hsc70 molecules required to initiate disassembly for wild type and H14 coats at pH 6.8 (Figure 5B, top and bottom panels, respectively). We model binding of Hsc70 to the intact coat with a maximum occupancy of one molecule per vertex (Xing et al., 2010) and a single rate constant for association ($k_1^+$) and dissociation ($k_1^-$) at any of the $N = 36$ vertices. The values of these rate constants ($k_1^+ = 0.07\ \mu M^{-1}\ s^{-1}$ and $k_1^- = 0.027\ s^{-1}$) were determined previously from Hsc70 binding curves measured at a range of Hsc70 concentrations (Böcking et al., 2011). We further assume that upon reaching a certain threshold level, $N_t$, of Hsc70 loading, the coat transitions to disassembly with a single rate limiting step of rate constant $k_2^+$. We fixed this rate constant at an average value of $k_2^+ = 0.13\ s^{-1}$ (see Experimental Procedures for details), similar to that determined independently before (Böcking et al., 2011). A numerical fit of the rate equations to the accumulation time distributions (Figure 5B, pink) obtained from several hundred single-particle uncoating traces yielded estimates of the threshold level $N_t$ as the only free model parameter. This threshold level represents the average number of Hsc70 molecules that need to be associated with the coat to trigger the transition to the disassembly phase. The total

number of Hsc70 molecules required for complete coat disassembly is larger because binding to the coat continues throughout the transition and disassembly steps.

The accumulation times of H14 coats (~10 s) were on average considerably shorter than those of wild type coats (~30 s). Kinetic modelling showed that a mutant coat had bound less than half of the amount of Hsc70 when it commits to uncoating ($N_t$ = 10) than does a wild-type coat ($N_t$ = 23). Disassembly (Figure 5B, green) proceeds as a single exponential decay, with a single rate-limiting step of rate constant $k_3^+$. Mutant coat disassembly was only marginally faster than wild-type coat disassembly. The complete kinetic model for accumulation and disassembly (Figure 5A) gave an excellent fit of the distributions of times for the entire uncoating reaction (Figure 5B, blue) when using the values for $N_t$ and $k_3^+$ determined as described above.

At pH 6.6, the uncoating kinetics for wild-type and mutant were indistinguishable (Figure S2) in contrast to the pronounced differences described above for pH 6.8. This observation is not surprising because the intrinsic stabilities of the wild-type and mutant coats are comparable at pH 6.6 whereas mutant coats are considerably less stable than wild type coats at pH 6.8 (Figure 3C). These analyses suggest that the Hsc70-driven uncoating of H14 coats proceeds with the same basic mechanism as for wild type coats but that the destabilised H14 coats require a lower threshold of Hsc70 binding to initiate disassembly.

## Dependence of the uncoating reaction on pH

To investigate further the effect of coat stability on the uncoating reaction, we varied the strength of the interactions between triskelions in the wild type clathrin lattice by varying the pH in the narrow range between pH 6.4 and pH 7.2 and following the uncoating reaction by single-particle fluorescence imaging. While disassembly is not synchronized between individual coats at a given pH, the average persistence time of the coat signal depends strongly on pH, as evident from the snapshots at 60 s after injection of auxilin(547-910) and Hsc70-ATP (Figure 6A) and the corresponding kymographs (Figure 6B) and single-particle traces (Figure 6C). The coats are very stable at pH 6.4. As a consequence, most coat signals (85%) remain high during the time of the imaging assay (200 s) while the disappearance of the remainder occurs only after a long delay of typically 30–50 s after injection of the uncoating reagents. As the pH is increased, the coat signals persist for increasingly shorter periods of time. At pH 7.2 the vast majority of coat signals (>90%) have decayed to background within 14 s after injection of the uncoating reagents. Concomitant with the acceleration of the uncoating reaction, there is a pronounced increase in the uncoating efficiency from pH 6.4 (15%) to pH 6.6 (88%); close to 100% uncoat at pH≥7.0 (Figure 6D), just as do clathrin cages in a bulk uncoating assay (Schmid and Rothman, 1985). The single-particle traces (Figure 6C) for the majority of coats at pH ≥ 6.6 showed the characteristic Hsc70 accumulation phase followed by rapid clathrin disassembly. In contrast, most clathrin signals observed at pH 6.4 remained constant or decreased only slowly despite efficient Hsc70 binding to a steady state level (Figure 6C). Thus, clathrin coats are effectively locked at pH 6.4, in agreement with previous observations at low pH (Braell et al., 1984; Xing et al., 2010), but undergo normal Hsc70-driven uncoating at pH ≥ 6.6.

To determine whether the differences in uncoating kinetics could be explained by an effect of pH on the rate of Hsc70 binding, we averaged the Hsc70 traces of coats that remain intact (Figure 6E). The mean Hsc70 binding curves determined at each pH were the same (Figure 6E), indicating that pH did not have a measurable effect on recruitment of Hsc70 between pH 6.6 and pH 7.2. Binding followed first order kinetics and the observed rate constant for Hsc70 association determined from a fit of the curves ($k_{obs} \approx 0.14\ s^{-1}$ for [Hsc70] = 1.3 μM, Figure 6E) was consistent with previously determined Hsc70 association rate constant, across a range of Hsc70 concentrations (Böcking et al., 2011). The pH-independence of the initial binding phase could also be seen from the mean intensity traces of coats that proceeded to disassembly (Figure 6F). These traces did not reach a plateau and the mean intensity decreased as soon as the signals of disassembling coats started to disappear. As expected this turning point occurred earlier at higher pH values. Nevertheless, the initial parts of the mean curves were superimposable. We conclude that the pronounced effects of pH on the outcome of the uncoating reaction is primarily due to coat stability and not driven by changes in Hsc70 recruitment.

Analysis of the accumulation time distributions measured at different pH (Figure 7, pink) with the kinetic model shown in Figure 5A yielded estimates of the threshold level $N_t$ as a function of pH (see Experimental Procedures for details of the model parameters). The pronounced shift of the accumulation time distributions to shorter times with increasing pH was reflected by a sharp drop in $N_t$ between pH 6.8 ($N_t$ = 22) and pH 7.2 ($N_t$ = 4) (Figures 7 and 8A). We determined the fluorescence intensity ratio of the Hsc70 and clathrin signals from all single-particle uncoating traces at the onset of coat disassembly to obtain a measure that is proportional to the number of bound Hsc70 molecules. The average Hsc70:clathrin intensity ratio (Figure 8B) confirmed the sharp drop with increasing pH in the amount of bound Hsc70 at the time of disassembly. Thus, the specific binding of a few Hsc70 molecules to the relatively unstable coat at pH 7.2 is sufficient to trigger the release of the first triskelion(s). Analysis of the kinetic data also showed that the uncoating rate increased as a function of pH (Figure 8C), demonstrating that the Hsc70-dependent uncoating proceeds more rapidly when coats are destabilised by higher pH.

## DISCUSSION

We have prepared histidine to glutamine mutants of clathrin heavy chain that at pH close to neutral assemble *in vitro* into clathrin/AP-2 coats more unstable than those assembled from wild-type clathrin. By using single-particle fluorescence imaging to examine the effect of pH on coat stability and the effect of coat stability on the kinetics of the Hsc70/ATP and auxilin-dependent uncoating reaction, we draw the following principal conclusions. (1) The pH dependence of coat stability derives at least in part from titration of histidine residues at the proximal-distal contact. (2) The number of structural perturbations required to remove triskelions from the coat and the rate of uncoating depend on the overall stability of the clathrin lattice: the less stable the coat, the smaller the number of Hsc70 molecules that must bind before uncoating can begin and the faster the disassembly. (3) Auxilin binding stabilizes coats. (4) Binding of Hsc70 to a vertex is independent of coat stability, and the effects of pH on the kinetics of uncoating do not result from differences in Hsc70 recruitment..

### Molecular interactions and coat stability

Guided by the structural model of the clathrin/AP-2 coat determined by cryoEM we identified six histidine residues of clathrin heavy chain located at the contact between proximal and distal legs of neighbouring triskelions in the coat and mutated them in pairs to glutamine to obtain three double mutants. All three double mutants assembled into stable D6 barrel coats at pH 6.5 with comparable yield to wild type clathrin, but mutant coats dissociated more readily than wild-type clathrin coats at pH ≥ 6.8. Assemblies formed with clathrin containing all six mutations were unstable when resuspended even at pH 6.5, a condition where wild type coats are extremely stable. These observations are consistent with the structural model prediction that the proximal-distal contact is the main determinant of coat stability on the basis of its strong structural conservation of the proximal/distal interface observed in the cryoEM structures of coats with two different symmetries and in native and auxilin-bound D6 barrels (Fotin et al., 2004b; Xing et al., 2010).

We speculate that the pH dependence of coat stability derives at least in part from titration of the interfacial histidine residues tested here: As the pH is increased from 6.2 to 7.2, fewer histidines protonate, decreasing the density of stabilising interactions. Removal of some of these interactions by mutation appears to have the same destabilising effect, which becomes measurable in our assay at pH ≥ 6.8. The uncoating reaction of in-vitro assembled coats is rapid at pH values that would be expected for the cytoplasm (pH 7.0 – 7.4) and kinetic modelling of the uncoating data at pH 7.2 show that binding of a few Hsc70 molecules is sufficient to initiate disassembly. This observation suggests that the clathrin lattice by itself is poised for disassembly at the pH values encountered in the cytosol, and rapid uncoating can be initiated with few perturbations.

At cytosolic pH only a (small) proportion of histidine residues are protonated, which leads to the following picture of coat stability: The coat as a whole is sufficiently stabilised by network of electrostatic interactions that are distributed randomly all over the coat. (Note that a D6 barrel coat with 36 triskelions contains 324 of the double histidine sites examined in this study.) The distribution of stabilising contacts may be dynamic allowing for structural fluctuations to occur while maintaining overall lattice integrity. In contrast the interactions mediated by protonated histidine residues would be insufficient to stabilise assemblies consisting of just a few triskelions. Thus, assembling structures would exhibit low stability at the very early stages of assembly and need to be stabilised by other factors to survive. The latter has been observed in growing clathrin coated pits at the plasma membrane. Clathrin coated pits that are not stabilised by cargo binding to adaptor proteins, especially AP-2 (Höning et al., 2005; Jackson et al., 2010), do not proceed to a complete clathrin coated vesicle but disassemble rapidly leading to the observation of so called abortive pits (Aguet et al., 2013; Ehrlich et al., 2004; Loerke et al., 2009).

### Mechanism of clathrin uncoating

Each triskelion is linked to its nearest neighbours by six proximal-distal contacts (Figure 1). Release of a triskelion or a group of triskelions may occur when a sufficient number of proximal-distal contacts break simultaneously. The probability of release increases when proximal-distal contacts are weakened by strain induced by Hsc70 binding.

Auxilin, originally isolated as a clathrin assembly protein, stabilises clathrin coats *in vitro* (Ahle and Ungewickell, 1990). It binds to one of three equivalent binding sites underneath the vertex where it makes contact with two ankle segments and a terminal domain of three different triskelions (Fotin et al., 2004a; Scheele et al., 2001). At high concentrations of auxilin, when all binding sites are occupied, it stabilises a conformational change at the junction between the ankle and distal segment of a triskelion leg (Fotin et al., 2004a). As expected, auxilin bound at high concentrations slowed the spontaneous release of triskelions from the coat consistent with the view that the interactions with three different triskelions effectively “cross-links” the coat. Thus, the free energy of auxilin binding more than offsets the energy cost of distorting the ankle crossing. During the uncoating reaction, Hsc70-ATP is recruited by the J-domain of auxilin to a location just underneath the ankle crossing where it can bind to the QLMLT motif in the unstructured C-terminal tail of clathrin heavy chain beneath the triskelion hub (Rapoport et al, 2008). Interaction with the clathrin substrate and the J-domain leads to ATP hydrolysis and closure of the substrate binding groove leading to tight association with clathrin and weakening of the contact with the J-domain of auxilin (Hartl & Hayer-Hartl, 2009). As a result, the triskelion involved in the clathrin:Hsc70 complex is captured in a conformation that is destabilised with respect to its contacts with the lattice due to displacement of the ankle of one or more triskelions forming the ankle crossing. This displacement leads to a strain that could propagate to destabilise the proximal-distal contact (Xing et al, 2010). At this point, auxilin may dissociate further destabilizing the lattice. Additional binding of Hsc70 to other vertices leads to weakening of a sufficient number of proximal-distal contacts so that the cooperative release of triskelions (the uncoating reaction) can now ensue.

We observed that the uncoating rate increased with increasing pH values. Mutation of histidine to glutamine residues at the proximal-distal contact has the same effect. Faster uncoating correlates with a lower threshold in the number of bound Hsc70 required for the cooperative release of triskelions. The coincident breaking of proximal-distal contacts may represent a rate-limiting step after association of a sufficient number of Hsc70 molecules. The point of disassembly is reached before Hsc70 binding has reached stochiometric levels of binding, whereby the average threshold for disassembly depends on the overall stability of the coat, which is determined by the strength of the proximal-distal contact. Thus, fewer perturbations induced by Hsc70 binding are required for disassembly when the proximal-distal contacts are intrinsically weakened by elevated pH or by the clathrin mutations used in this study.

Based on recent biochemical studies (Young et al., 2013), it has been proposed that the clathrin light chains might be involved in the uncoating reaction, because the efficiency with which auxilin can mediate the uncoating reaction decreases in their absence. Our observations show that the increased uncoating with the mutant coats do not depend on light chains, since they bound equally well to wild type and histidine mutant triskelions.

To conclude, our results confirm two predictions. The first concerns the source of lattice stability in the clathrin coat. We identified a set of histidine residues, at the invariant interface between the proximal and distal legs of two triskelions, that contribute to the assembly and stability of the clathrin lattice. The second prediction concerns the mechanism

of chaperone-mediated uncoating. A key component of the proposed uncoating mechanism is trapping by Hsc70 of destabilizing fluctuations in the clathrin lattice. Weakening interactions in the coat should decrease the number of trapped distortions required to disassemble the lattice. The effect of the histidine mutations on uncoating susceptibility is consistent with this prediction.

## EXPERIMENTAL PROCEDURES

### Proteins

Fluorescent clathrin was reconstituted from recombinant rat clathrin heavy chain trimers and recombinant rat clathrin light chain (LCa1 D203E/C218S) labeled with maleimide-derivatised fluorophores (Alexa Fluor 488, Alexa Fluor 568 or DyLight 649) as described (Böcking et al., 2011). Bovine Hsc70 was expressed, purified and labeled at an added C-terminal cysteine residue using Alexa Fluor-C5-maleimide (Böcking et al., 2011). Bovine auxilin(547-910) containing the J-domain and clathrin-binding sites was expressed and purified as described (Rapoport et al., 2008).

### Coat formation

Recombinant clathrin triskelions were mixed with an adaptor fraction isolated from calf brain and highly enriched in AP-2 (Rapoport et al., 2008) at a ratio of 3:1 (w/w). The mixture was dialysed against coat formation solution (50 mM MES pH 6.5, 100 mM NaCl, 2 mM EDTA, 0.5 mM DTT) at 4 °C for 14 h with one solution exchange. After removal of aggregates by low-speed centrifugation (TLA 100.4 rotor, 12000 rpm, 10 min, 4 °C), the coats were harvested by ultracentrifugation (TLA 100.4 rotor, 65000 rpm, 14–16 min, 4 °C) and resuspended in coat formation solution at a concentration of ~1 mg/mL.

### Electron microscopy

Diluted solutions of the coats were applied to carbon-coated electron microscopy grids immediately after cleaning by glow discharge and blotted with filter paper. The samples were stained with freshly prepared solution of 1.2% (w/v) uranyl acetate, blotted and air-dried. Electron micrographs were obtained using a Tecnai $G^2$ Spirit BioTWIN at a primary magnification of 30,000. Coat diameters were measured using ImageJ and data sets were compared with one-way analysis of variance and Tukey's multiple comparison test using Prism (GraphPad Software).

### Surface chemistry and flow cell preparation

Glass cover slips were cleaned by sonication in ethanol (30 min) and 1 M NaOH (30 min) followed by rinsing with ultrapure water, drying and treatment in a glow-discharge unit. The glass surface was covered with a solution of the co-polymer PLL(20)-g[3.4]-PEG(2)/PEG(3.4)-biotin (20%) (Susos AG) in PBS (1 mg/mL) for 30 min and rinsed with ultrapure water. The surface was then covered with a solution of streptavidin (0.2 mg/mL in 20 mM Tris pH 7.5, 2 mM EDTA, 50 mM NaCl, 0.03% $NaN_3$, 0.025% Tween 20, 0.2 mg/mL bovine serum albumin), incubated for 30 min and rinsed with ultrapure water. The microfluidic flow cell was assembled by clamping a polydimethylsiloxane device with

microfluidic channels (80 μm high and 800 μm wide) onto the modified glass cover slip. A syringe pump was used to pull solutions through the microfluidic channels.

### Capture of clathrin coats and TIRF microscopy

The biotinylated antibody CVC.6 directed against clathrin LCa was immobilised on the surface of the cover slip modified with streptavidin. Fluorescent clathrin coats were flowed through the microfluidic channel and captured onto the surface of the coverslip via the antibody. A brief pulse (1–2 μL of ~0.1 mg/mL coats in coat formation solution) was sufficient to capture several hundred coats per field of view. Images were acquired sequentially for the different fluorophores using an inverted microscope (Zeiss 200M) with TIRF slider and Alpha Plan-Apo 100× objective (1.46 NA). Solid state lasers (488 nm, 561 nm and 640 nm) were used for excitation and an electron multiplying CCD camera (QuantEM 512 SC, Photometrics) for detection of fluorescence emission.

### Clathrin coat stability assay

Wild-type and mutant clathrin coats each labeled with different fluorophores were captured onto the surface of the cover slip and exposed to buffer solutions (50 mM imidazole, 100 mM KCl, 2 mM $MgCl_2$) adjusted to increasing pH values (pH 6.4 to 7.8 in steps of 0.2 pH units). Solutions were exchanged in the microfluidic channels by flowing 30 μL buffer solution at a flow rate of 30 μL/min. A single fluorescence image in each channel was recorded at the end of an incubation period (1 min) at each pH value to determine the loss of fluorescence signal of wild-type and mutant clathrin coats. Under these imaging conditions photobleaching was negligible.

### Single-particle uncoating assay

Auxilin was bound to the coats immediately after their capture onto the cover slip by flowing a solution of 0.05 mg/mL (1.3 μM) auxilin(547-910) in uncoating solution (20 mM imidazole pH 6.8, 100 mM KCl, 2 mM $MgCl_2$) through the microfluidic channel. To initiate the uncoating reaction, a mixture containing Hsc70-AF568 at various concentrations, 0.02 mg/mL (0.5 μM) auxilin(547-910) and 2 mM ATP in uncoating solution was injected into the microfluidic channel at a flow rate of 100 μL/min. Image acquisition was started just prior to injection of the uncoating reagents. Images were acquired with an exposure of 2–10 ms and a frequency of 1–2 frames per second. The antioxidant trolox (2 mM) and an oxygen-quenching system consisting of protocatechuic acid (2.5 mM) and protocatechuate-3,4-dioxygenase (0.25 U/mL) were used to minimize photobleaching (Aitken et al., 2008).

### Image analysis and kinetic modeling

Fluorescence images were analyzed using algorithms coded in MATLAB (The MathWorks, Inc.). The fluorescence intensity traces for clathrin and Hsc70 were calculated by Gaussian fitting of the corresponding diffraction-limited signals in each channel. The beginning ($t = 0$) of the reaction was defined as the arrival time of the labelled Hsc70-ATP at the cover slip surface and determined from the appearance of fluorescence background in the Hsc70 channel. We then used an algorithm based on automated step fitting of each single-particle

trace (Kerssemakers et al., 2006) to determine the time point at which the clathrin signal started to decay and the time point at which the clathrin signal had reached a stable level close to the background. Coats that undergo an uncoating reaction were defined as those traces exhibiting a phase of rapid signal disappearance. Kinetic modeling to determine the critical number of Hsc70 molecules ($N_t$) required to initiate disassembly was carried out as described previously (Böcking et al., 2011). We found little variation in the value of $k_2^+$ obtained by numerical fits of the rate equations to the accumulation time distributions for uncoating experiments conducted at pH 6.8 ($k_2^+ = 0.13 \pm 0.05\ s^{-1}$) and fixed $k_2^+$ at the average value for analysis of the data in Figure 5. Further, the value of $k_2^+$ was only weakly dependent on pH in the range between pH 6.6 and pH 7.0. Numerical fits of the accumulation time distributions with $k_2^+$ as a free model parameter yielded estimates of $k_2^+ = 0.1\ s^{-1}$, $0.13\ s^{-1}$ and $0.16\ s^{-1}$ for pH 6.6, 6.8 and 7.0, respectively. Fits with a fixed value of $k_2^+ = 0.13\ s^{-1}$ described these distributions equally well and yielded estimates for $N_t$ of 24, 22 and 9 for pH 6.6, 6.8 and 7.0, respectively. A higher value of $k_2^+ = 0.38\ s^{-1}$ was required for the fit of the accumulation time distribution at pH 7.2. The uncoating kinetics and estimates for $N_t$ determined for wild type coats labelled with either Alexa Fluor 488 or DyLight649 were indistinguishable showing that the type of fluorophore used for clathrin labelling did not affect the outcome of the single-particle uncoating assay.

## Supplementary Material

Refer to Web version on PubMed Central for supplementary material.

## Acknowledgments

We thank S.C. Harrison for input into the design of the mutants, discussions and editorial help, E. Marino for maintaining the Imaging Resource and members of our laboratories for discussions. TB was supported by a fellowship from the Human Frontier Science Program Organization. FA was supported by a fellowship from the Swiss National Science Foundation. MB was supported by a fellowship from the European Molecular Biology Organization. This work was supported by NIH grants GM-075252 and U54 AI057159 (New England Regional Center of Excellence in Biodefense and Emerging Infectious Disease, Core Imaging Facility) to TK and Australian Research Council grant FT100100411 to TB. Designed experiments: TB, TK. Data analysis and modelling: FA, TB. Carried out experiments: AY (clathrin mutants), IR (protein expression and purification, coat formations), JCZ (pH stability assay), MB (EM, pH stability assay), TB (uncoating assay), TK (EM). Wrote the manuscript: TB, TK. Discussed results and commented on the manuscript: all authors.

## References

Aguet F, Antonescu CN, Mettlen M, Schmid SL, Danuser G. Advances in Analysis of Low Signal-to-Noise Images Link Dynamin and AP2 to the Functions of an Endocytic Checkpoint. Developmental cell. 2013

Ahle S, Ungewickell E. Auxilin, a newly identified clathrin-associated protein in coated vesicles from bovine brain. J Cell Biol. 1990; 111:19–29. [PubMed: 1973169]

Aitken CE, Marshall RA, Puglisi JD. An oxygen scavenging system for improvement of dye stability in single-molecule fluorescence experiments. Biophys J. 2008; 94:1826–1835. [PubMed: 17921203]

Barouch W, Prasad K, Greene L, Eisenberg E. Auxilin-induced interaction of the molecular chaperone Hsc70 with clathrin baskets. Biochemistry. 1997; 36:4303–4308. [PubMed: 9100026]

Böcking T, Aguet F, Harrison SC, Kirchhausen T. Single-molecule analysis of a molecular disassemblase reveals the mechanism of Hsc70-driven clathrin uncoating. Nat Struct Mol Biol. 2011; 18:295–301. [PubMed: 21278753]

Braell WA, Schlossman DM, Schmid SL, Rothman JE. Dissociation of clathrin coats coupled to the hydrolysis of ATP: role of an uncoating ATPase. J Cell Biol. 1984; 99:734–741. [PubMed: 6146631]

Brodsky FM, Chen CY, Knuehl C, Towler MC, Wakeham DE. Biological basket weaving: formation and function of clathrin-coated vesicles. Ann Rev Cell Dev Biol. 2001; 17:517–568. [PubMed: 11687498]

Crowther RA, Pearse BM. Assembly and packing of clathrin into coats. J Cell Biol. 1981; 91:790–797. [PubMed: 7328122]

Edeling MA, Smith C, Owen D. Life of a clathrin coat: insights from clathrin and AP structures. Nat Rev Mol Cell Biol. 2006; 7:32–44. [PubMed: 16493411]

Ehrlich M, Boll W, Van Oijen A, Hariharan R, Chandran K, Nibert ML, Kirchhausen T. Endocytosis by random initiation and stabilization of clathrin-coated pits. Cell. 2004; 118:591–605. [PubMed: 15339664]

Fotin A, Cheng Y, Grigorieff N, Walz T, Harrison SC, Kirchhausen T. Structure of an auxilin-bound clathrin coat and its implications for the mechanism of uncoating. Nature. 2004a; 432:649–653. [PubMed: 15502813]

Fotin A, Cheng Y, Sliz P, Grigorieff N, Harrison SC, Kirchhausen T, Walz T. Molecular model for a complete clathrin lattice from electron cryomicroscopy. Nature. 2004b; 432:573–579. [PubMed: 15502812]

Guan R, Han D, Harrison SC, Kirchhausen T. Structure of the PTEN-like region of auxilin, a detector of clathrin-coated vesicle budding. Structure. 2010; 18:1191–1198. [PubMed: 20826345]

Hartl FU, Hayer-Hartl M. Converging concepts of protein folding in vitro and in vivo. Nat Struct Mol Biol. 2009; 16:574–581. [PubMed: 19491934]

Höning S, Ricotta D, Krauss M, Späte K, Spolaore B, Motley A, Robinson M, Robinson C, Haucke V, Owen DJ. Phosphatidylinositol-(4,5)-bisphosphate regulates sorting signal recognition by the clathrin-associated adaptor complex AP2. Molecular cell. 2005; 18:519–531. [PubMed: 15916959]

Jackson LP, Kelly BT, McCoy AJ, Gaffry T, James LC, Collins BM, Höning S, Evans PR, Owen DJ. A large-scale conformational change couples membrane recruitment to cargo binding in the AP2 clathrin adaptor complex. Cell. 2010; 141:1220–1229. [PubMed: 20603002]

Keen JH. Clathrin and associated assembly and disassembly proteins. Ann Rev Biochem. 1990; 59:415–438. [PubMed: 1973890]

Kerssemakers JWJ, Munteanu EL, Laan L, Noetzel TL, Janson ME, Dogterom M. Assembly dynamics of microtubules at molecular resolution. Nature. 2006; 442:709–712. [PubMed: 16799566]

Kirchhausen T. Clathrin. Ann Rev Biochem. 2000; 69:699–727. [PubMed: 10966473]

Kirchhausen T, Harrison SC. Protein organization in clathrin trimers. Cell. 1981; 23:755–761. [PubMed: 7226229]

Loerke D, Mettlen M, Yarar D, Jaqaman K, Jaqaman H, Danuser G, Schmid SL. Cargo and dynamin regulate clathrin-coated pit maturation. PLoS Biology. 2009; 7:e57. [PubMed: 19296720]

Massol RH, Boll W, Griffin AM, Kirchhausen T. A burst of auxilin recruitment determines the onset of clathrin-coated vesicle uncoating. Proc Natl Acad Sci USA. 2006; 103:10265–10270. [PubMed: 16798879]

Morgan JR, Jiang J, Oliphint PA, Jin S, Gimenez LE, Busch DJ, Foldes AE, Zhuo Y, Sousa R, Lafer EM. A role for an Hsp70 nucleotide exchange factor in the regulation of synaptic vesicle endocytosis. The Journal of neuroscience: the official journal of the Society for Neuroscience. 2013; 33:8009–8021. [PubMed: 23637191]

Musacchio A, Smith CJ, Roseman AM, Harrison SC, Kirchhausen T, Pearse BM. Functional organization of clathrin in coats: combining electron cryomicroscopy and X-ray crystallography. Mol Cell. 1999; 3:761–770. [PubMed: 10394364]

Pearse BM, Crowther RA. Structure and assembly of coated vesicles. Ann Rev Biophys Biophys Chem. 1987; 16:49–68. [PubMed: 2885011]

Rapoport I, Boll W, Yu A, Böcking T, Kirchhausen T. A motif in the clathrin heavy chain required for the Hsc70/auxilin uncoating reaction. Mol Biol Cell. 2008; 19:405–413. [PubMed: 17978091]

Scheele U, Kalthoff C, Ungewickell E. Multiple interactions of auxilin 1 with clathrin and the AP-2 adaptor complex. J Biol Chem. 2001; 276:36131–36138. [PubMed: 11470803]

Schlossman DM, Schmid SL, Braell WA, Rothman JE. An enzyme that removes clathrin coats: purification of an uncoating ATPase. J Cell Biol. 1984; 99:723–733. [PubMed: 6146630]

Schmid SL, Rothman JE. Enzymatic dissociation of clathrin cages in a two-stage process. J Biol Chem. 1985; 260:10044–10049. [PubMed: 2862146]

Schuermann JP, Jiang J, Cuellar J, Llorca O, Wang L, Gimenez LE, Jin S, Taylor AB, Demeler B, Morano KA, et al. Structure of the Hsp110:Hsc70 nucleotide exchange machine. Mol Cell. 2008; 31:232–243. [PubMed: 18550409]

Smith CJ, Grigorieff N, Pearse BM. Clathrin coats at 21 A resolution: a cellular assembly designed to recycle multiple membrane receptors. EMBO J. 1998; 17:4943–4953. [PubMed: 9724631]

Ungewickell E, Ungewickell H, Holstein SE, Lindner R, Prasad K, Barouch W, Martin B, Greene LE, Eisenberg E. Role of auxilin in uncoating clathrin-coated vesicles. Nature. 1995; 378:632–635. [PubMed: 8524399]

Vigers GP, Crowther RA, Pearse BM. Three-dimensional structure of clathrin cages in ice. EMBO J. 1986; 5:529–534. [PubMed: 3635476]

Xing Y, Böcking T, Wolf M, Grigorieff N, Kirchhausen T, Harrison SC. Structure of clathrin coat with bound Hsc70 and auxilin: mechanism of Hsc70-facilitated disassembly. EMBO J. 2010; 29:655–665. [PubMed: 20033059]

Ybe JA, Brodsky FM, Hofmann K, Lin K, Liu SH, Chen L, Earnest TN, Fletterick RJ, Hwang PK. Clathrin self-assembly is mediated by a tandemly repeated superhelix. Nature. 1999; 399:371–375. [PubMed: 10360576]

Young A, Stoilova-McPhie S, Rothnie A, Vallis Y, Harvey-Smith P, Ranson N, Kent H, Brodsky FM, Pearse BMF, Roseman A, et al. Hsc70-induced Changes in Clathrin-Auxilin Cage Structure Suggest a Role for Clathrin Light Chains in Cage Disassembly. Traffic. 2013; 14:987–996. [PubMed: 23710728]

- Invariant interface at the edges of the clathrin coat contribute to lattice stability
- Proximal and distal legs of two adjacent triskelions contribute to the interface
- Histidine residues at the interface help stabilize the clathrin lattice
- Sub-stoichiometric amount of Hsc70 molecules mediates lattice disassembly

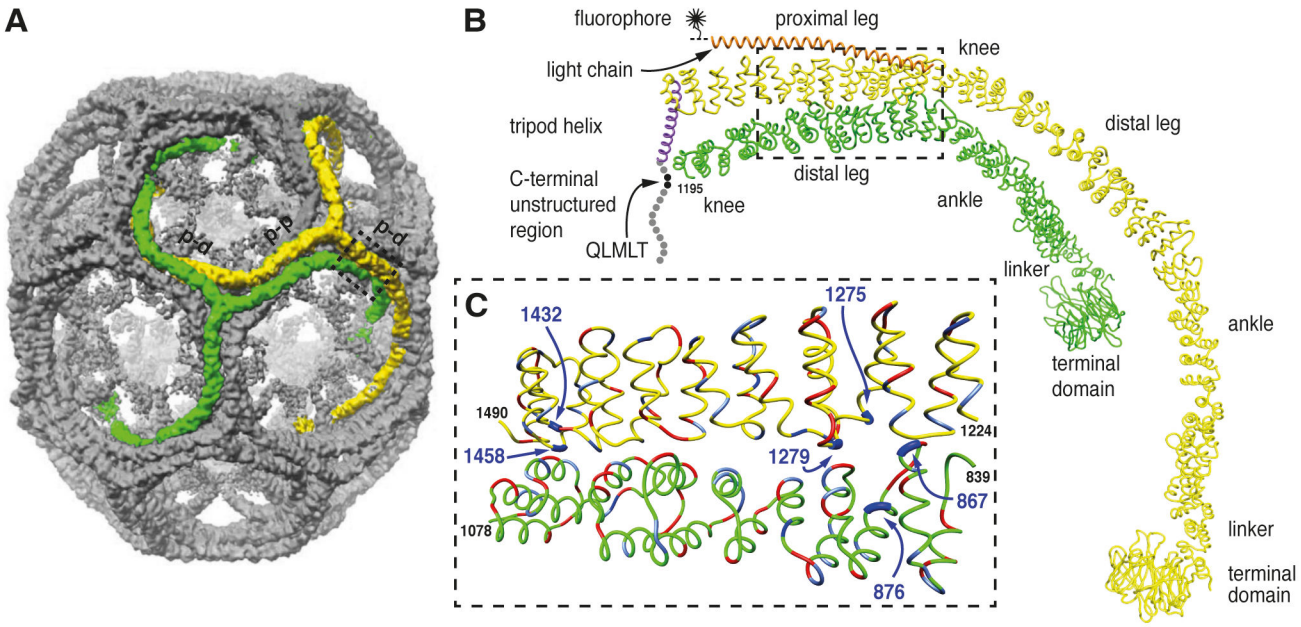


**Figure 1. Location of histidine residues at the contacts between proximal and distal segments of neighboring triskelions**

**A.** Image reconstruction of a clathrin/AP-2 coat in the D6 barrel form (Fotin et al., 2004b). The contacts between parallel proximal and distal segments of the triskelions highlighted in green and yellow are indicated (p-d). The antiparallel proximal segments of the triskelions highlighted in green and yellow are indicated (p-p).

**B.** α-Carbon traces of single legs from neighboring triskelions (yellow and green, indicated by the dashed box in A) showing the invariant contact between parallel proximal and distal heavy chain segments viewed from the side. The heavy chain molecule shown in green comprises residues 1-1195 (includes part of the knee, distal leg, ankle, linker and terminal domain). The yellow heavy chain is associated with the central helix of its bound light chain (orange) and the α-helix of its trimerization domain forming part of the C-terminal tripod of the triskelion (purple). The disordered region of the heavy chain (residues 1630-1675) is indicated by the spheres with the binding site for Hsc70 (QLMLT motif) shown in black. The central helical segment of clathrin light chain is shown in orange. For imaging the light chain was labeled with a fluorophore at a single cysteine residue C-terminal to the helical segment. **C.** Close-up view of the interface between the proximal segment of the yellow heavy chain and the distal segment of the green heavy chain viewed from the side. The histidine residues mutated in this study are shown in dark blue and indicated by the arrows. Negatively charged residues are shown in red and positively charged residues are shown in light blue.

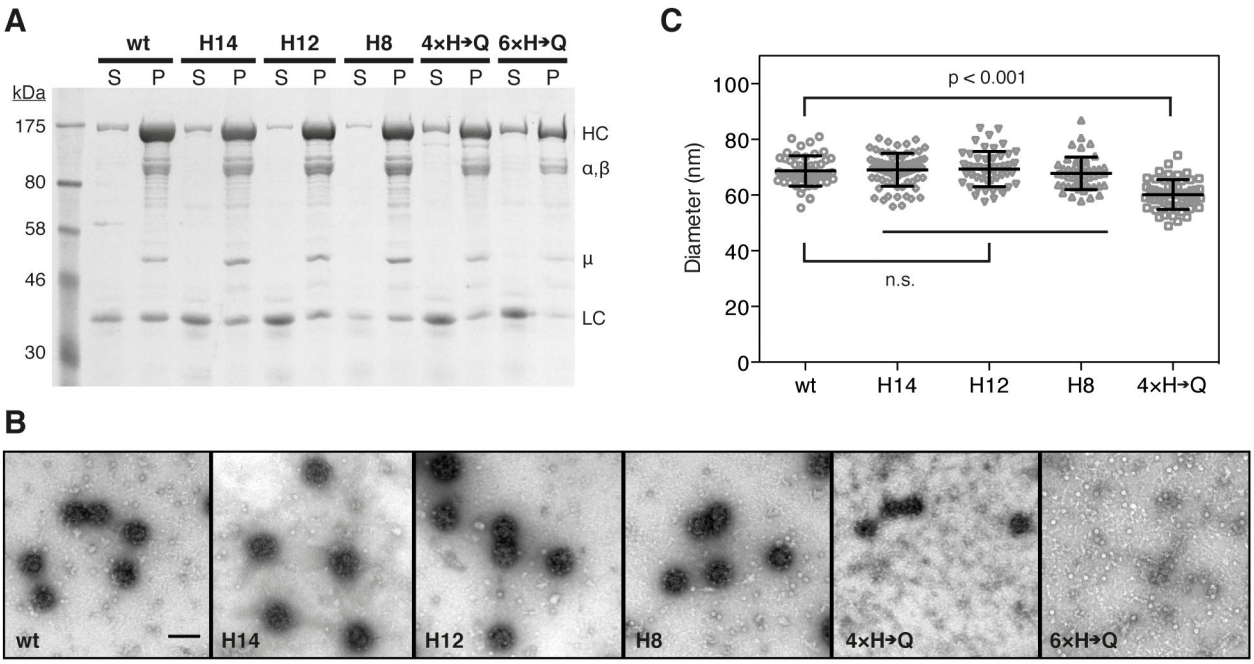


**Figure 2. Clathrin coat assembly using wild type and histidine clathrin mutants**

**A.** SDS PAGE and Coomassie Blue analysis of the high speed centrifugation supernatant (S) and pellet (P) fractions of clathrin/AP-2 coats. HC, clathrin heavy chain; α,β and μ-chain of AP-2; LC, clathrin light chain.

**B.** Electron micrographs of fields of negatively stained (1.2% uranyl acetate) clathrin/AP-2 coats assembled with wild type clathrin heavy chain or histidine mutants. Bar, 100 nm.

**C.** Diameters of clathrin coats assembled with wild type clathrin heavy chain or histidine mutants determined from the EM images, $N \geq 50$ coats were measured for each coat preparation; mean ± s.d.

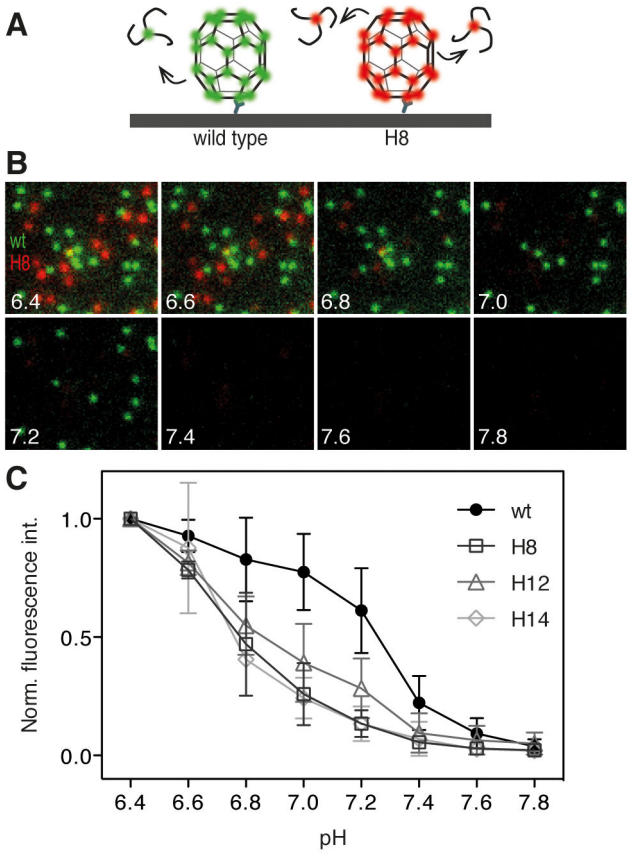


**Figure 3. Clathrin coats assembled with clathrin heavy chain histidine double mutants are less stable than wild type at higher pH**

**A.** Schematic representation of the fluorescence microscopy assay to measure coat stability. Clathrin/AP-2 coats assembled from fluorescent clathrin trimers were captured with an antibody directed against LCa1 onto a chemically modified coverslip and imaged by TIRF microscopy before and after exposure to buffer solutions of increasing pH.

**B.** Representative images of clathrin/AP-2 coats assembled with wild type clathrin labeled with LCa-AF488 and mutant H8 labeled with LCa-DL649 after exposure to buffer solutions in the pH range from pH 6.4 to pH 7.8.

**C.** pH stability curves for clathrin/AP-2 coats assembly with wild type clathrin or the histidine double mutants H14, H12 or H8.

See also Figure S1.

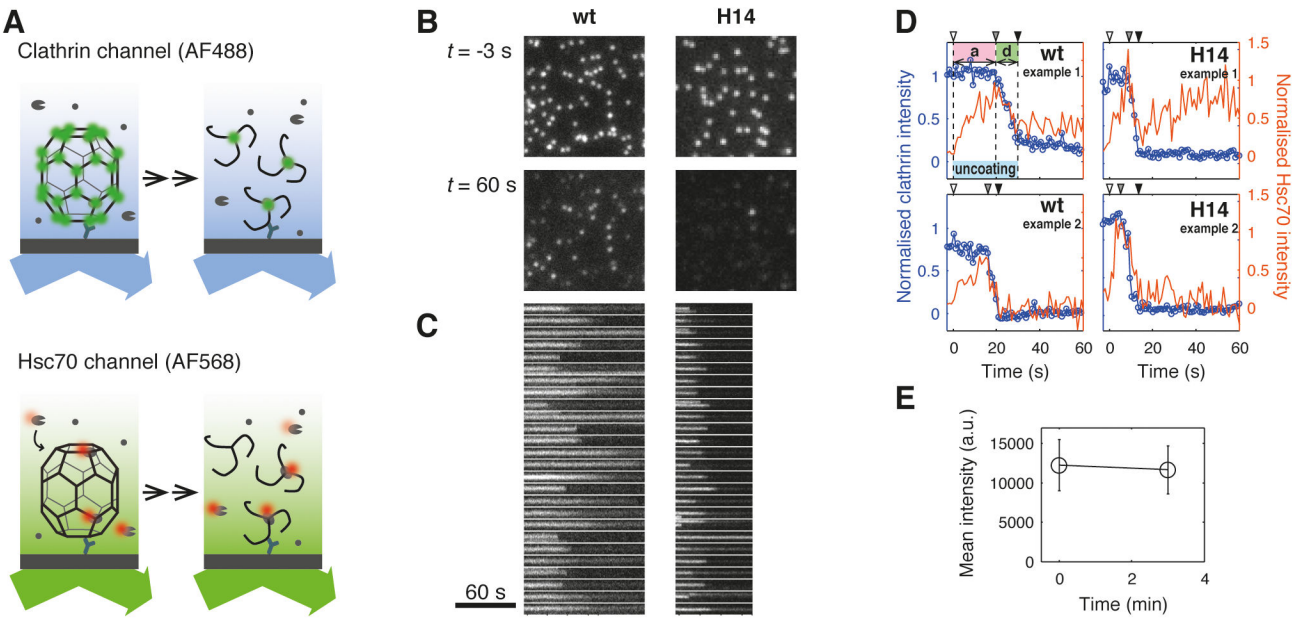


**Figure 4. Single-particle uncoating assay of wild-type and H14 mutant coats**

**A.** Schematic representation of the single-particle uncoating assay.

**B.** Frames of the uncoating time series (120×120 pixel region for wild type coats and 60×60 pixel region with 2×2 binning for H14 coats) showing the diffraction-limited signals from fluorescent coats loaded with auxilin(547-910) before (top) and 60 s after addition of 1.0 μM Hsc70-ATP (bottom) at pH 6.8.

**C.** Kymographs of the clathrin signal originating from coats contained in the images shown in B.

**D.** Representative uncoating traces for clathrin/AP-2 coats assembled with wild type or H14 clathrin. The arrow heads indicate the arrival of Hsc70-ATP (t = 0, open arrowhead), the start (grey arrowhead) and the end (black arrowhead) of the disassembly phase. The intensity trace of the clathrin signal is shown in blue and the intensity trace of the Hsc70 signal is shown in orange.

**E.** Fluorescence intensities (mean ± standard deviation) of H14 clathrin/AP-2 coats before (top, $N$ = 581 coats) and after (bottom, $N$ = 611 coats) exposure to buffer solution (pH 6.8) containing 1.3 μM auxilin(547-910) for 3 min.

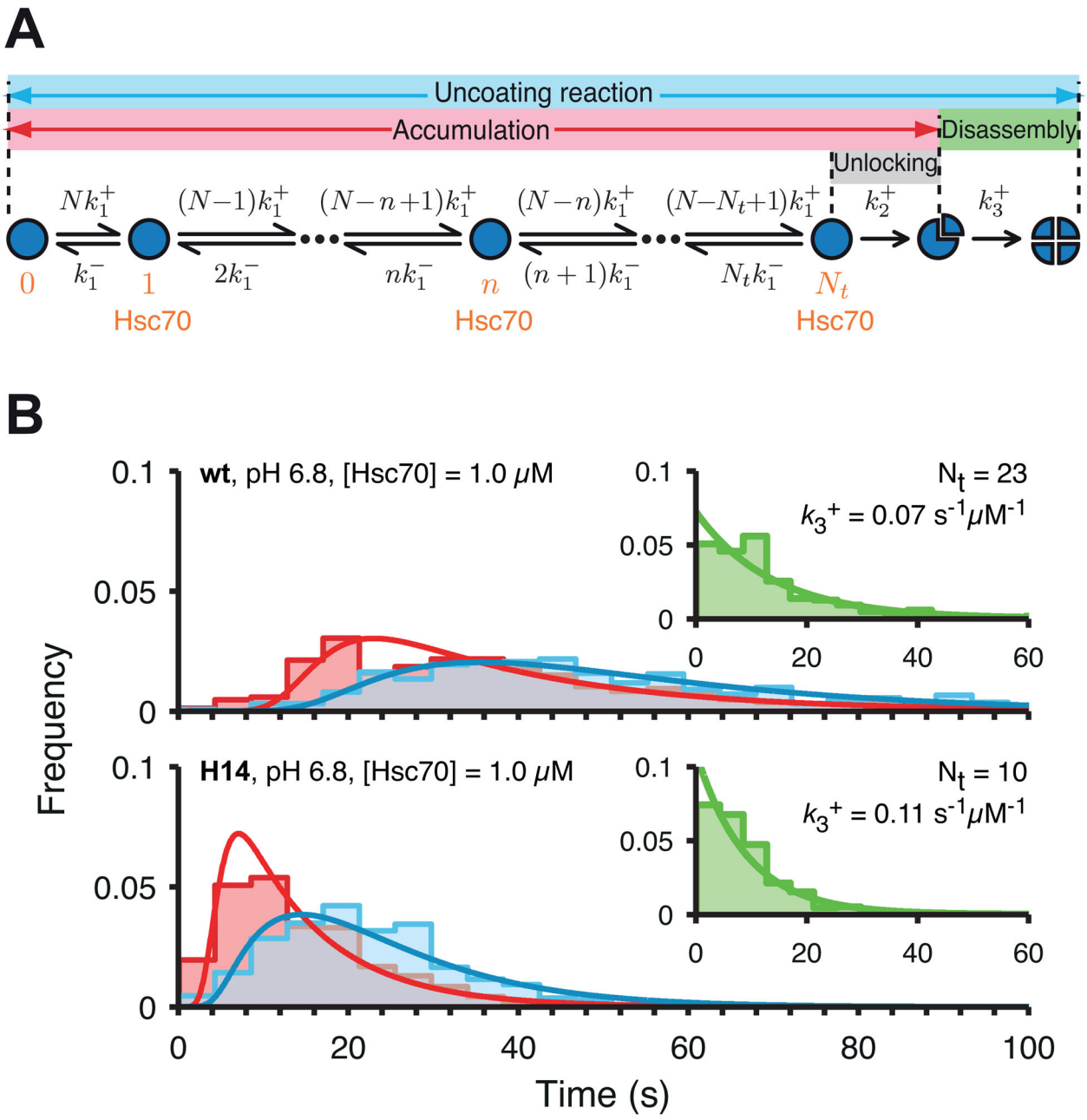


**Figure 5. Kinetic model of the uncoating reaction**

**A.** Scheme of the kinetic model.

**B.** Distributions of Hsc70 accumulation times (red), disassembly times (green) and the full uncoating reaction times (blue) overlaid with fits of the kinetic model. The uncoating reaction was carried out with wild type or H14 mutant coats at pH 6.8 in the presence of 1.0 μM Hsc70.

See also Figure S2.

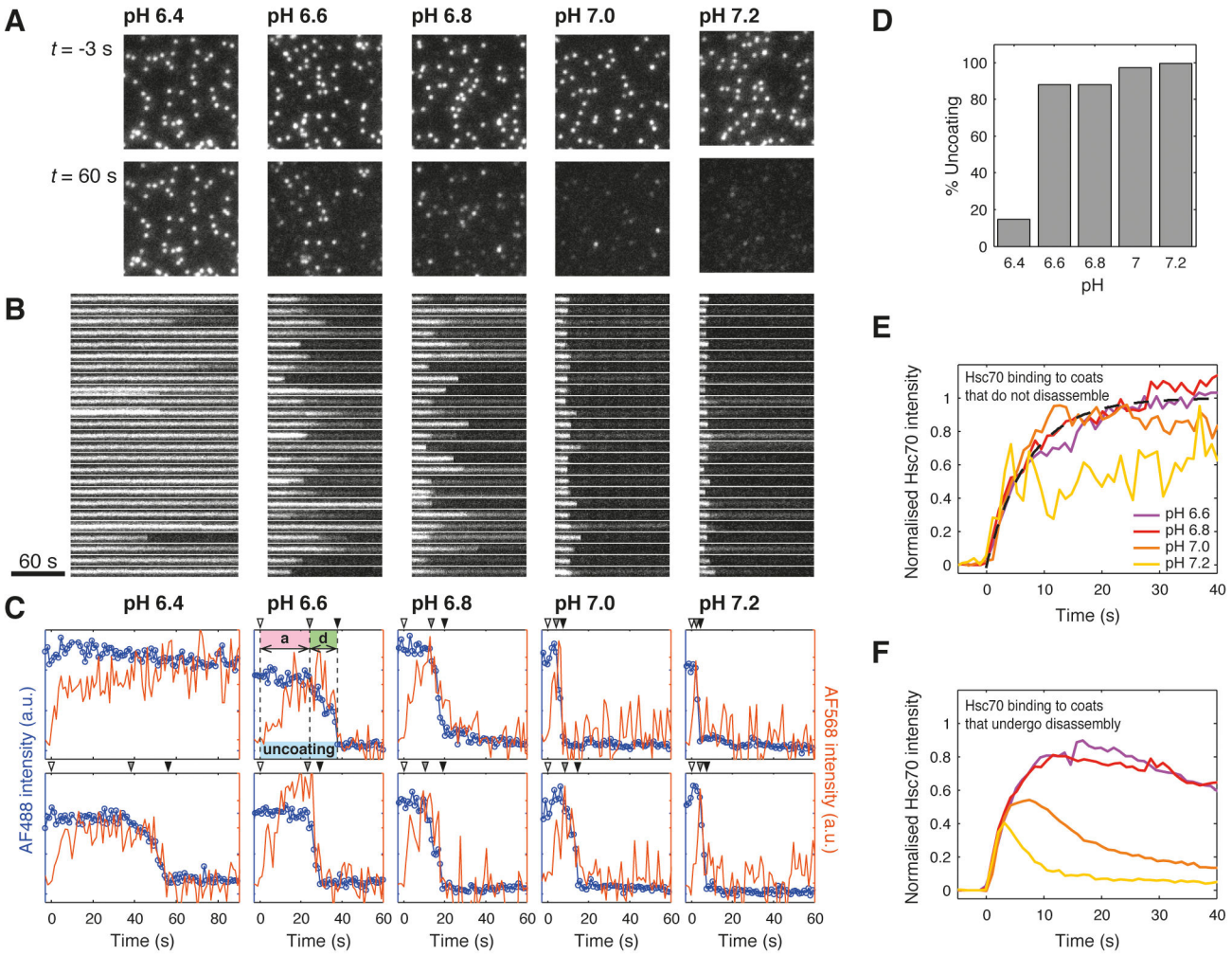


**Figure 6. Single-particle uncoating assay at various pH values**

**A.** Frames of the uncoating time series (120×120 pixel region from a 512×512 pixel image) showing the diffraction-limited signals from AF-488 coats loaded with auxilin(547-910) before (top) and 60 s after addition of 1.0 μM Hsc70-ATP (bottom) at pH values between 6.4 and 7.2.

**B.** Kymographs of the clathrin signal originating from coats contained in the images shown in panel A.

**C.** Representative uncoating traces for clathrin/AP-2 coats showing binding of Hsc70 to the coats during the accumulation phase (“a”) followed by rapid coat disassembly (“d”). The arrow heads indicate the arrival of Hsc70-ATP (*t* = 0, open arrowhead), the start (grey arrowhead) and the end (black arrowhead) of the disassembly phase. The intensity trace of the clathrin signal is shown in blue and the intensity trace of the Hsc70 signal is shown in orange.

**D.** Uncoating efficiency of wild type clathrin/AP-2 coats between pH 6.4 and pH 7.2.

**E/F.** Hsc70 binding to the coats during the accumulation phase is not pH-dependent. The colored traces correspond to the average binding curves of Hsc70-ATP to coats in uncoating assays conducted between pH 6.6 and pH 7.2 for coats that remain intact (shown in F;

average of $N$ = 86, 93, 17, 3 traces for pH 6.6, 6.8, 7.0, 7.2, respectively) or those that undergo uncoating (shown in F; average of $N$ = 624, 683, 617, 846 traces for pH 6.6, 6.8, 7.0, 7.2, respectively). The dotted line represents a fitted association curve.

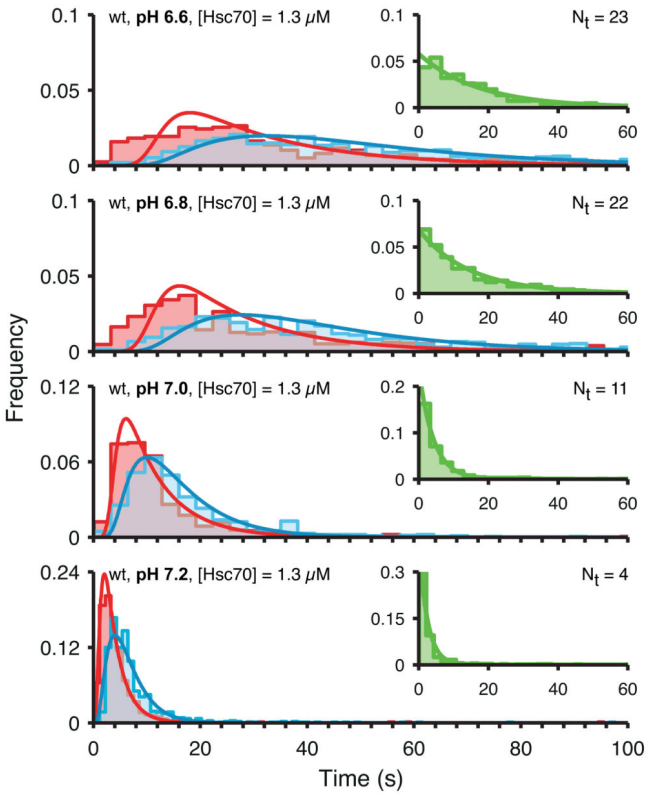


**Figure 7. pH dependence of the uncoating kinetics**

Distributions of Hsc70 accumulation times (red), disassembly times (green) and the times of the entire uncoating reaction (blue) overlaid with fits of the kinetic model. The uncoating reaction was carried out with wild type coats at various pH values in the range between pH 6.6 and 7.2 in the presence of 1.3 μM Hsc70.

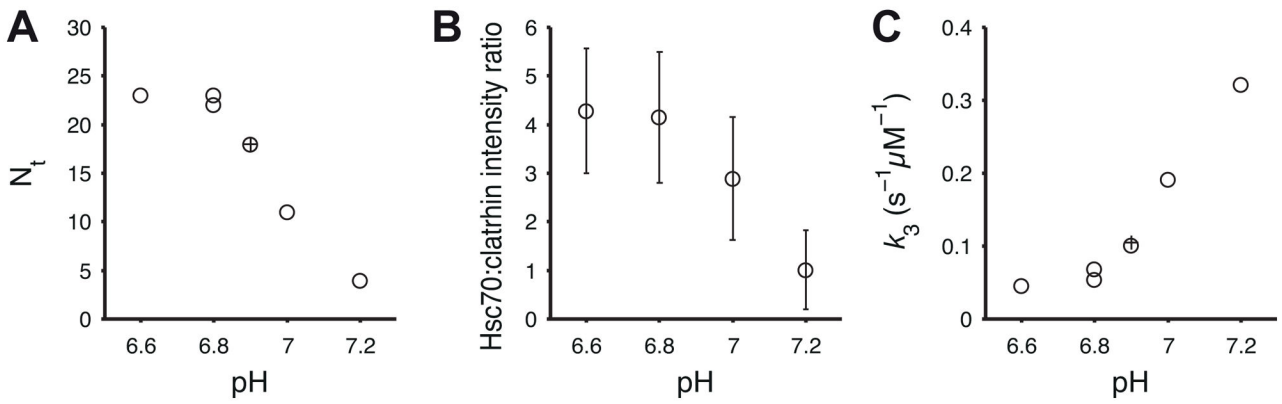


**Figure 8. Destabilized clathrin lattices require less Hsc70 to initiate disassembly and fall apart faster**

**A.** Number of Hsc70 molecules per coat ($N_t$) required to commit the reaction to disassembly as a function of pH determined by kinetic modeling; ○, data from Figure 5, Figure 7 and control experiments; +, average $N_t$ determined previously across a range of Hsc70 concentrations (Böcking et al., 2011).

**B.** Average ratio of the Hsc70:clathrin fluorescence intensities determined for each trace at the time point just prior to coat disassembly (average of $N$ = 624, 683, 617, 846 traces for pH 6.6, 6.8, 7.0, 7.2, respectively)

**C.** Rate constant $k_3^+$ describing the disassembly phase as a function of pH determined by kinetic modeling; ○, data from Figure 5, Figure 7 and control experiments; +, average $k_3^+$ determined previously across a range of Hsc70 concentrations (Böcking et al., 2011).